








Article

In Situ Synthesis of Magnetic Poly(DMAEAB-co-NIPAm)@Fe₃O₄ Composite Hydrogel for Removal of Dye from Water

Zhi Chen ^{1,2} , Xia Song ¹ , Wilson Wee Mia Soh ¹ , Yuting Wen ¹ , Jingling Zhu ¹ , Miao Zhang ¹ 
and Jun Li ^{1,*} 

¹ Department of Biomedical Engineering, National University of Singapore, 7 Engineering Drive 1, Singapore 117574, Singapore; z.chen@cqu.edu.cn (Z.C.); a0045788@u.nus.edu (X.S.); wilson.soh@u.nus.edu (W.W.M.S.); bieweny@nus.edu.sg (Y.W.); erizhuj@nus.edu.sg (J.Z.); zhangmiao@u.nus.edu (M.Z.)

² School of Chemistry and Chemical Engineering, Chongqing University of Technology, Chongqing 400054, China

* Correspondence: jun-li@nus.edu.sg or jun-li@u.nus.edu; Tel.: +65-65167273

Abstract: Water pollution by toxic substances, such as dye molecules, remains a major environmental problem that needs to be solved. In the present work, the magnetic composite hydrogel based on the poly(2-(methacryloyloxy)-N-(2-hydroxyethyl)-N,N-dimethylethan-1-aminium bromide-co-N-isopropylacrylamide) copolymer with incorporated Fe₃O₄ particles ((poly(DMAEAB-co-NIPAm)@Fe₃O₄)) was prepared by an in situ synthesis technique for the efficient removal of dye molecules from water. The successfully synthesized magnetic hydrogel was characterized by FTIR, XRD, TGA, and TEM. The removal efficiency of the anionic dye bromophenol blue (BPB) and the cationic dye rhodamine B (RDM) by the prepared hydrogel adsorbents was evaluated. Various adsorption parameters, including the concentration of adsorbents and adsorption time, were also investigated. The results showed that the synthesized magnetic hydrogel had excellent BPB removal performance compared to the removal of RDM. The optimum adsorbent concentration for 0.5 mM BPB solution was approximately 0.5 g/L, and the removal efficiency was more than 99%. The kinetics data of BPB removal fitted well into the pseudo-2nd-order model, indicating that BPB dye adsorption involves chemical adsorption and physical adsorption. In addition, recycling studies were conducted to examine the reusability of the magnetic hydrogel for BPB removal for up to five cycles and the hydrogel could be reused without losing its high removal efficiency. The magnetic hydrogel poly(DMAEAB-co-NIPAm)@Fe₃O₄ with high removal efficiency, good selectivity, and reusability shows great potential for the removal of anionic dyes in wastewater treatment.

Keywords: magnetic hydrogel; composite; adsorption; bromophenol blue; water treatment



Citation: Chen, Z.; Song, X.; Soh, W.W.M.; Wen, Y.; Zhu, J.; Zhang, M.; Li, J. In Situ Synthesis of Magnetic Poly(DMAEAB-co-NIPAm)@Fe₃O₄ Composite Hydrogel for Removal of Dye from Water. *Gels* **2021**, *7*, 201. <https://doi.org/10.3390/gels7040201>

Academic Editor: Bin Xue

Received: 30 September 2021

Accepted: 2 November 2021

Published: 5 November 2021

Publisher's Note: MDPI stays neutral with regard to jurisdictional claims in published maps and institutional affiliations.



Copyright: © 2021 by the authors. Licensee MDPI, Basel, Switzerland. This article is an open access article distributed under the terms and conditions of the Creative Commons Attribution (CC BY) license (<https://creativecommons.org/licenses/by/4.0/>).

1. Introduction

The dyestuff industry is important to the economy and many other industrial sectors, because a large number of synthetic dyes are applied in textile, leather, printing, paper, cosmetic, and food industries. Unfortunately, 10–15% of the dyes are eventually discharged into industrial effluents, becoming major environmental pollutants [1,2]. These dye molecules or their metabolites may be highly toxic, potentially carcinogenic, and even cause organic mutations or allergies in exposed organisms. They not only pollute the environment but also cross the entire food chain [3–5]. At present, the main treatment methods for dye wastewater are chemical oxidation, electro-coagulation, membrane filtration, biodegradation, flocculation, and adsorption [6–11]. Compared with other treatment methods, the adsorption method has become the most effective technique to remove dye or heavy metal ions from wastewater in the chemical, pharmaceutical, biological, and environmental industries because of its advantages of being eco-friendly, simple to operate, low energy consuming, and exhibiting great performance [12,13]. Therefore, it is an

inevitable trend to develop highly selective and environmentally friendly adsorptions with high adsorption capacity.

Hydrogels, as one of the most important adsorbents, have been widely used as superabsorbent materials, water shutoff agents for petroleum recovery, filling materials for biological soft tissues, water-proof concrete additives, etc., in many fields such as health, chemical industry, biomedicine, and architecture [14–16]. There have been increasing studies to develop hydrogels for pollutant removal from water based on host–guest interactions. One example is a β -cyclodextrin-based hydrogel to remove organic pollutants from water [17]. At present, progress has also been made in the preparation of stimulus-responsive hydrogels, such as the thermosensitive hydrogel, the pH-responsive hydrogel, the magnetic responsive hydrogel, and the electric field responsive hydrogels [18–27]. Thermoresponsive hydrogels are among the most widely studied stimuli-responsive hydrogels. Poly(*N*-isopropylacrylamide) (PNIPAm) is an ideal thermoresponsive polymer because of its phase transition properties in response to temperature changes, and it has been used in functional materials for biological and biomedical applications and environmental sustainability [28–35]. A PNIPAm-based thermoresponsive smart adsorption system has been developed for efficient copper ion removal from water [18]. Magnetic hydrogels have also been developed for adsorption of contaminants from water because they could be easily separated from the solution by an external magnetic field [30]. Therefore, the molecular structure design of environmental-stimulus-responsive hydrogel is highly useful for improving the adsorption capacity and selectivity of the adsorbents by making use of specific interactions between the adsorbents and the adsorbates.

In this work, we synthesized and characterized a magnetic composite hydrogel based on poly(2-(methacryloyloxy)-*N*-(2-hydroxyethyl)-*N,N*-dimethylethan-1-aminium bromide-co-*N*-isopropylacrylamide) (poly(DMAEAB-co-NIPAM)) cationic copolymers with incorporated Fe_3O_4 particles using a simple in situ synthesis method. The magnetic (poly(DMAEAB-co-NIPAM)@ Fe_3O_4) composite hydrogel was investigated for its effectiveness as an adsorbent in the removal of the anionic dye bromophenol blue (BPB) and the cationic dye rhodamine B (RDM). The effects of variables, such as adsorbent concentrations (g/L) and adsorption time (min), were studied and optimized. In addition, the adsorption process was further explored by fitting the data into adsorption kinetic models. The regeneration properties of the hydrogel were also investigated, demonstrating its potential reusability and simple fast separation characteristics in the adsorption and desorption of the dye molecules.

2. Experimental Section

2.1. Materials

N-isopropyl acrylamide (NIPAm, A.R. grade) was obtained from Tokyo Chemical Industry (TCI) Co., LTD., Tokyo, Japan. 2-Dimethylaminoethyl methacrylate (DMAEMA, A.R. grade), 2-bromoethanol (A.R. grade), *N,N'*-methylenebisacrylamide (MBA, C.P. grade), iron(III) chloride (FeCl_3 , reagent grade, $\geq 97\%$), sodium sulfite (Na_2SO_3 , A.R. grade), potassium persulfate (KPS, ACS grade, $\geq 99\%$), bromophenol blue (BPB, electrophoresis reagent grade), rhodamine B (RDM, reagent grade, $\geq 95\%$), and ammonium hydroxide solution (ACS reagent, 28–30%, NH_3 basis) were purchased from Sigma–Aldrich Chemical Company, Inc. (St. Louis, MO, USA) Other reagents were all analytical grade, and all solutions were prepared with deionized (DI) water (the electrical resistivity was $18 \text{ M}\Omega\cdot\text{cm}$ at 25°C , Millipore Direct-Q[®]5UV water purification system).

2.2. Synthesis of Poly(DMAEAB-co-NIPAm) Hydrogel

The poly(DMAEAB-co-NIPAm) hydrogel was synthesized with a one-pot method by free radical copolymerization of DMAEMA and NIPAm in aqueous medium, using 2-bromoethanol as the cationic quaternary ammonium reagent, MBA as the crosslinker, and KPS as the initiator. In brief, DMAEMA (3.4659 g, 0.02 mol), NIPAm (2.4790 g, 0.02 mol) monomers, and 2-bromoethanol (2.7217 g, 0.02 mol) in 50 mL of water was stirred in a

150 mL three-neck round-bottom flask; MBA (0.1181 g, 2 wt% with respect to the weight of DMAEMA and NIPAm) was added into the reaction mixture and maintained at 50 °C for 4 h with nitrogen gas. Then, the KPS initiator (59.1 mg, 1 wt% based on weight percentages of DMAEMA and NIPAm) was dissolved in 10 mL of water and added into the reaction mixture under nitrogen gas. The polymerization reaction continued for 4 h at 50 °C until a colorless transparent poly(DMAEAB-co-NIPAm) hydrogel was obtained. Next, the obtained hydrogel was shattered and immersed in DI water for 3 days (water was changed every 24 h) to remove the unreacted or soluble materials. Finally, the hydrogel was freeze-dried to afford the poly(DMAEAB-co-NIPAm) hydrogel powder and designated as P100. A control hydrogel, P0, was synthesized following the same procedures for preparing P100, without the addition of 2-bromoethanol.

2.3. Synthesis of Poly(DMEMAB-co-NIPAm)@Fe₃O₄ Magnetic Hydrogel

The magnetic hydrogel was synthesized according to the protocol adapted from the literature [36]. Briefly, 0.25 g FeCl₃ in 20 mL of DI water was mixed with 1 mL of 4.8 wt% sodium sulfite aqueous solution and stirred vigorously at room temperature for 1 h under nitrogen atmosphere to reach equilibrium. One gram of P100 hydrogel powder was added into the prepared iron cation solution and swelled for 24 h to absorb all the solution. Subsequently, 5 mL of ammonium hydroxide solution was added to and rinsed with the swollen hydrogel for 4 h. Then, the swollen hydrogel, which changed to a black color, was washed with water until the pH of the solution became neutral and dried at 70 °C in a vacuum oven to obtain the P100@Fe₃O₄ magnetic hydrogel. A control hydrogel, P0@Fe₃O₄, was prepared following the same procedures for preparing P100@Fe₃O₄, using P0 instead of P100.

2.4. Characterizations

Fourier transform infrared (FTIR) spectra of samples in potassium bromide (KBr) pellets were recorded on an Agilent Cary 600 spectrophotometer (Agilent Co., Ltd., Palo Alto, CA, USA) in the range of 400–4000 cm⁻¹. Scanning electron microscope (SEM) and energy-dispersive X-ray spectroscopy (EDS) studies were carried out using a Regulus 8230 (HITACHI Co., Ltd., Tokyo, JPN) equipped with an Ultim Extreme (Oxford Instruments, Oxford, UK). Thermogravimetric analysis (TGA) thermograms were measured with a thermogravimetric analyzer (NETZSCH STA 2500, Selb, Bavaria, Germany). The scanning temperature range was from room temperature to 700 °C and the heating rate was 10 °C/min. The morphology and size of the particles were characterized by transmission electron microscopy (TEM, JEM-2010F, JEOL Co., Ltd., Tokyo, JPN). The samples were dispersed in absolute ethanol by ultrasonication and dripped on copper mesh and measured in the dry state with 200 kV. The crystalline structure of the samples was determined using X-ray diffraction (XRD, Bruker Single Crystal D8 Venture, Bruker Co., Ltd., Karlsruhe, Germany). The scan range (2θ) was from 20 to 65°, and the scanning step frequency was 1 (°)/min. The ultraviolet–visible (UV–Vis) measurements of the solutions were tested using a UV–Vis spectrophotometer (UV-2600, SHIMADZU Corp., Kyoto, Japan).

2.5. Dye Removal Experiments

In the batch adsorption studies to investigate the optimum adsorbent concentrations for BPB and RDM dye removal, different amounts (0–50 mg) of the non-magnetic or magnetic hydrogel adsorbents were added separately into 20 mL of the BPB dye solution (0.5 mM, 350 mg/L) or RDM dye solution (0.01 mM, 5 mg/L) in a glass vial and stirred for 120 min. In the kinetic studies of dye removal, 0.42 g/L of the adsorbent was used for BPB solution (initial concentration of 350 mg/L), and 0.62 g/L of the adsorbent was used for RDM solution (initial concentration of 5 mg/L) for a period of 2 h. After a predetermined interval of time, the P0@Fe₃O₄ and P100@Fe₃O₄ hydrogels were separated from the solution by an external magnet, while the P0 and P100 hydrogels were separated by centrifugation. The supernatant was taken to measure its absorbance to determine the

dye concentration after adsorption. All experiments were conducted at 25 °C. A series of dye solutions with different concentrations were prepared to produce a standard curve by measuring the absorbance with a UV–Vis spectrophotometer from 400 to 700 nm at a scanning speed of 2 nm/s at room temperature. The chemical structures of the dyes and their UV–Vis spectra at various concentrations are shown in Figure 1. The wavelength of maximum absorbance, λ_{\max} , was 591 nm for BPB and 554 nm for RDM. The standard curve equations for the dyes were also generated: BPB dye, $y = 60.564x + 0.0403$ with $R^2 = 0.9991$; RDM dye, $y = 143.65x + 0.06$ with $R^2 = 0.9978$.

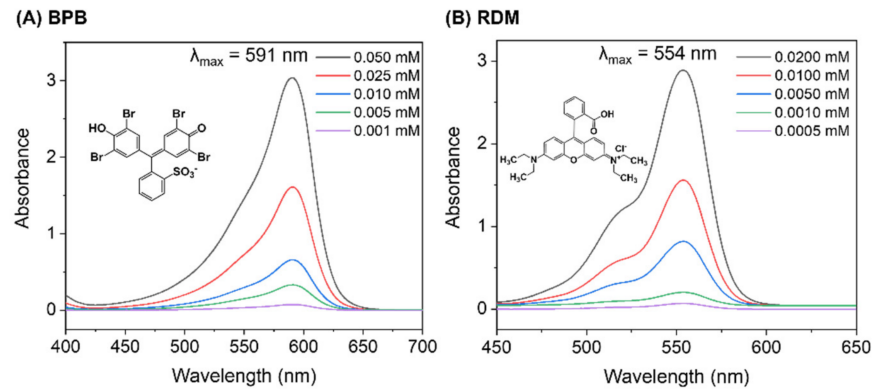


Figure 1. The chemical structures of BPB dye (A) and RDM dye (B) and their UV–Vis spectra at various concentrations.

The residual concentration of the dye solution was determined using the standard curve. Equations (1) and (2) were used to calculate the equilibrium adsorption capacity (q_e) and the removal efficiency (E) of dye, respectively.

$$q_e = \frac{(C_0 - C_e)V}{m} \quad (1)$$

$$E = \frac{C_0 - C_e}{C_0} \times 100\% \quad (2)$$

where C_0 and C_e (mg/L) are the initial and equilibrium concentration of the dye, respectively. V (L) is the solution volume, and m (g) is the mass of adsorbent used.

The kinetics data for dye adsorption were fitted into pseudo-1st-order and pseudo-2nd-order models with the following expressions (i.e., (3) and (4)), respectively:

$$\ln(q_e - q_t) = \ln q_e - k_1 t \quad (3)$$

$$\frac{t}{q_t} = \frac{1}{k_2 q_e^2} + \frac{t}{q_e} \quad (4)$$

where q_e and q_t are the dye adsorption capacity (mg g^{-1}) at equilibrium and time t , respectively, and k_1 (min^{-1}) and k_2 ($\text{g mg}^{-1} \text{min}^{-1}$) are the pseudo-1st-order and pseudo-2nd-order rate constants, respectively.

2.6. Recycling Studies

After an adsorption experiment using 1 g/L of the adsorbents in 0.5 mM BPB solution, the desorption of BPB from the magnetic hydrogel P100@Fe₃O₄ and the non-magnetic hydrogel P100 was carried out in weakly acidic solutions (pH = 6) at 25 °C to regenerate the adsorbents before they were used again in subsequent cycles. The washing time needed to desorb BPB dye from the magnetic hydrogel P100@Fe₃O₄ and the non-magnetic hydrogel P100 was 2 and 5 min, respectively. The adsorption/desorption process was conducted five times.

3. Results and Discussion

3.1. Synthesis of Poly(DMAEAB-co-NIPAm)@Fe₃O₄ Magnetic Composite Hydrogel

The poly(DMAEAB-co-NIPAm) (P100) non-magnetic hydrogel and poly(DMAEAB-co-NIPAm)@Fe₃O₄ (P100@Fe₃O₄) magnetic hydrogel were successfully synthesized according to the protocol described in Figure 2. The control samples, poly(DMAEMA-co-NIPAm) (P0) non-magnetic hydrogel and poly(DMAEMA-co-NIPAm)@Fe₃O₄ (P0@Fe₃O₄) magnetic hydrogel, were also synthesized following the same protocol but without the addition of 2-bromoethanol. The synthesis parameters for the copolymer hydrogels are summarized in Table 1.

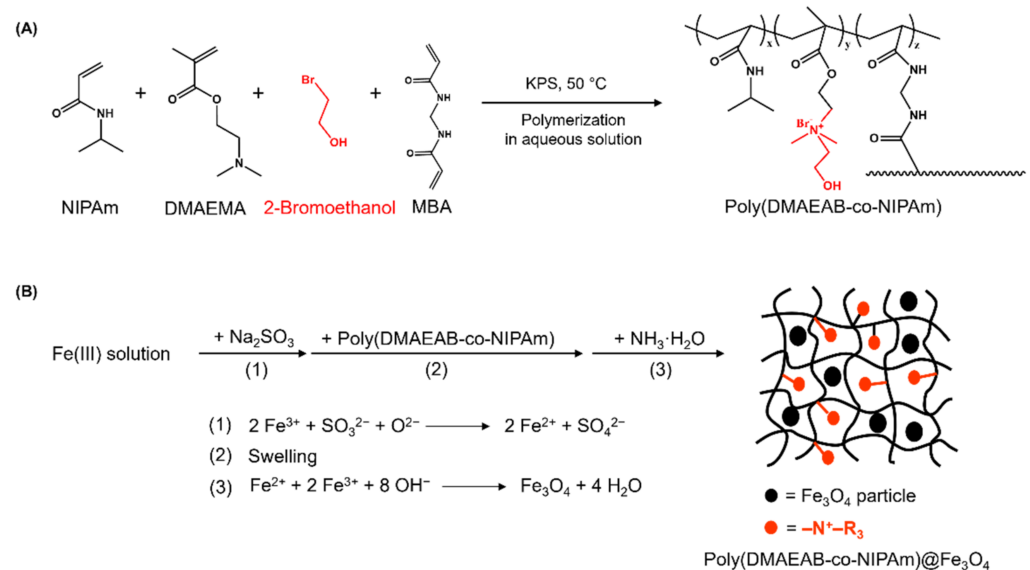


Figure 2. Synthesis scheme of (A) poly(DMAEAB-co-NIPAm) (P100) non-magnetic hydrogel and (B) poly(DMAEAB-co-NIPAm)@Fe₃O₄ (P100@Fe₃O₄) magnetic hydrogel.

Table 1. Synthesis parameters and thermal stability properties of the hydrogels.

Hydrogel	Feed Ratios for Copolymer Hydrogels				Thermal Stability Parameters ¹	
	DMAEMA	NIPAm	2-Bromoethanol	MBA	T _{10%} weight loss (°C)	T _{50%} weight loss (°C)
P0	1	1	-	0.03	202.6	338.1
P0@Fe ₃ O ₄	1	1	-	0.03	233.1	384.1
P100	1	1	1	0.03	139.5	272.7
P100@Fe ₃ O ₄	1	1	1	0.03	221.4	350.1

¹ Data obtained from TGA analysis.

3.2. Characterizations of Poly(DMAEAB-co-NIPAm)@Fe₃O₄ Magnetic Composite Hydrogel

The FTIR spectra of the synthesized hydrogels are shown in Figure 3. The peaks around 1650 cm⁻¹ and 1386 cm⁻¹ and around 2970 cm⁻¹ and 2827 cm⁻¹ corresponded to the characteristic absorption peaks of C=O, -CH(CH₃)₂ and C-H of NIPAm of the P0 and P100 hydrogels, respectively. The peaks around 1730 cm⁻¹ and 1150 cm⁻¹ corresponded to the characteristic absorption peaks of C=O and C-O of DMAEMA of the hydrogel. After the introduction of Fe₃O₄ particles, the characteristic absorption peaks of each functional group were still present, but the intensity was weakened in the magnetic hydrogel P0@Fe₃O₄ and P100@Fe₃O₄, and the characteristic peaks of Fe-O were very obvious, near 570 cm⁻¹. Therefore, the FTIR analysis showed that the non-magnetic hydrogels (i.e., P0 and P100) and the magnetic hydrogels (i.e., P0@Fe₃O₄ and P100@Fe₃O₄) were successfully prepared.

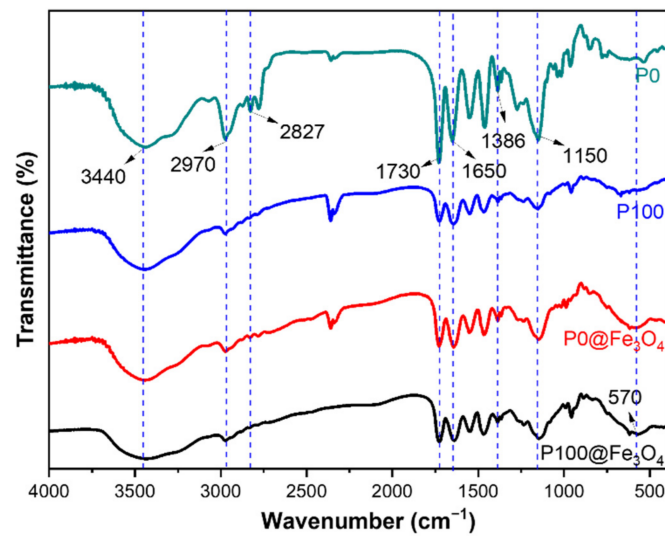


Figure 3. FTIR spectra of the non-magnetic hydrogels (i.e., P0 and P100) and the magnetic hydrogels (i.e., P0@Fe₃O₄ and P100@Fe₃O₄).

The XRD patterns of the magnetic hydrogels P0@Fe₃O₄ and P100@Fe₃O₄ were measured to analyze their crystalline structures and compositions (Figure 4 (left)). There were obvious diffraction peaks at 30.2, 35.5, 43.4, 53.9, 57.1, and 62.8° that responded to the (220), (311), (400), (422), (511), and (440) crystal planes of cubic phase Fe₃O₄, respectively [37]. These results indicate that the Fe₃O₄ particles were successfully introduced into the magnetic hydrogels P0@Fe₃O₄ and P100@Fe₃O₄, and the organic components had no effect on the crystallinity of Fe₃O₄. Moreover, the magnetic hydrogel particles had good dispersions in deionized water (Figure 4 (right)). When the magnet was close to the dispersions, obvious magnetic separation occurred quickly. P100@Fe₃O₄ particles were attracted to the wall of the vial near the magnetic field, which showed that the prepared Fe₃O₄ particles inside the hydrogel had good paramagnetism. After removing the magnet, the P100@Fe₃O₄ hydrogel particles re-dispersed into the solution under ultrasonication or shaking.

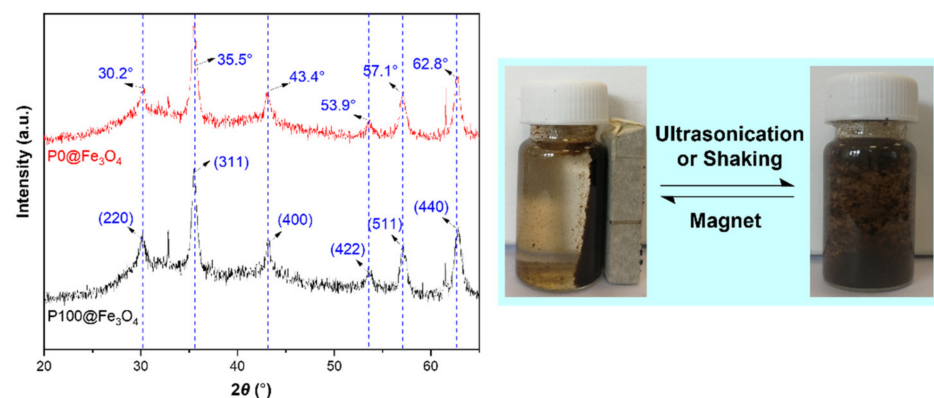


Figure 4. XRD diffractograms of the magnetic hydrogels (left) and photographs of P100@Fe₃O₄ particles in deionized water (right).

The thermal stability of the P0, P100, P0@Fe₃O₄, and P0@Fe₃O₄ hydrogels was analyzed using TGA, and the thermograms are shown in Figure 5. The corresponding thermal stability parameters are listed in Table 1. In Figure 5, the weight loss might be attributed to H₂O elimination from the hydrogel at a temperature of approximately 230 °C. The weight loss between 230 and 570 °C was mainly due to the decomposition of poly(DMEMAB-co-NIPAm)'s main chain molecules in the hydrogel. The 50% weight loss of the hydrogel P100,

P100@Fe₃O₄, P0, and P0@Fe₃O₄ were observed at 272.7, 350.1, 338.1, and 384.1 °C, respectively. The data confirmed that the magnetic hydrogels (i.e., P100@Fe₃O₄ and P0@Fe₃O₄) were more stable than the non-magnetic hydrogels (i.e., P100 and P0). This might be attributed to the incorporation of Fe₃O₄ into the hydrogel network.

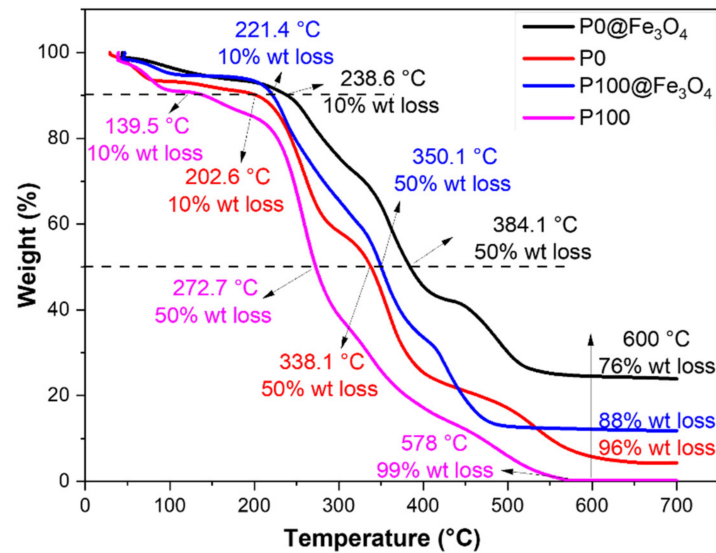


Figure 5. TGA thermograms of the non-magnetic hydrogels (i.e., P0 and P100) and the magnetic hydrogels (i.e., P0@Fe₃O₄ and P100@Fe₃O₄).

The TEM images of the magnetic hydrogel P100@Fe₃O₄ particles are shown in Figure 6. They reveal the presence of Fe₃O₄ particles in this hydrogel, which were less than 10–20 nm in size. It was further proved that the magnetic hydrogel P100@Fe₃O₄ was successfully prepared.

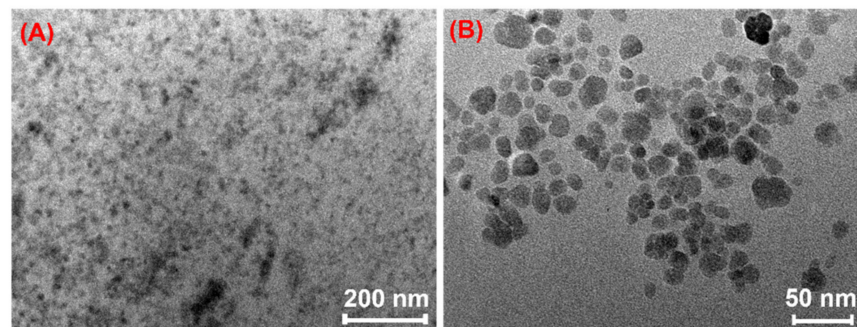


Figure 6. TEM images of P100@Fe₃O₄ at different scales: (A) Scale bar = 200 nm; (B) Scale bar = 50 nm.

3.3. Dye Removal Experiments

The dye removal efficiencies of P0@Fe₃O₄ and P100@Fe₃O₄ adsorbents were analyzed. They were investigated for removing BPB and RDM dyes from aqueous solutions to study the adsorption parameters. P0 and P100 were used as control samples to compare the effect of the magnetic properties on removal efficiencies. Furthermore, the adsorption time and adsorbents dosage on the BPB and RDM removal from aqueous solutions was analyzed. Batch adsorption studies were carried out to investigate the optimum adsorbent concentrations for BPB dye removal. In this study, different concentrations of the adsorbents were prepared by adding different amounts (0–50 mg) into 20 mL of BPB dye solution (0.5 mM, 350 mg/L) or RDM dye solution (0.01 mM, 5 mg/L) and stirred for 120 min. A magnet was used to separate the P0@Fe₃O₄ and P100@Fe₃O₄ adsorbents from the solution, while the P0 and P100 adsorbents were separated by centrifugation.

Figure 7A shows the removal efficiencies of BPB dye from aqueous solution by the different concentrations of the adsorbents. It was found that increasing the adsorbent concentration increased the BPB removal efficiency. The BPB removal efficiency reached 98.5% at optimum concentrations of 0.455, 0.625, and 0.79 g/L of P100, P100@Fe₃O₄, and P0@Fe₃O₄, respectively. It was found that P0@Fe₃O₄ hydrogel had a very high removal efficiency at a concentration of 0.79 g/L, whereas P0 hydrogel could only achieve 53.3% removal efficiency at a similar concentration. This might be attributed to the increase in N⁺ positive charge density, which could significantly increase the ionic interactions with BPB dye molecules [38]. In addition, the incorporation of Fe₃O₄ particles might contribute to the increase in the adsorption active sites, which was conducive to the adsorption of dye molecules [39]. Another factor to consider was the molecular structure of the P100. As indicated by the SEM image of P100 (Figure 8A), P100 hydrogel had a 3D-layered structure and large surface area, which was helpful for fast adsorption of dye molecules. Based on the above reasons, the order of the performance of the four hydrogels in removing BPB dye was approximated to be P100 > P100@Fe₃O₄ > P0@Fe₃O₄ > P0. The schematic illustration for BPB removal by the magnetic hydrogel P100@Fe₃O₄ is shown in Figure 9.

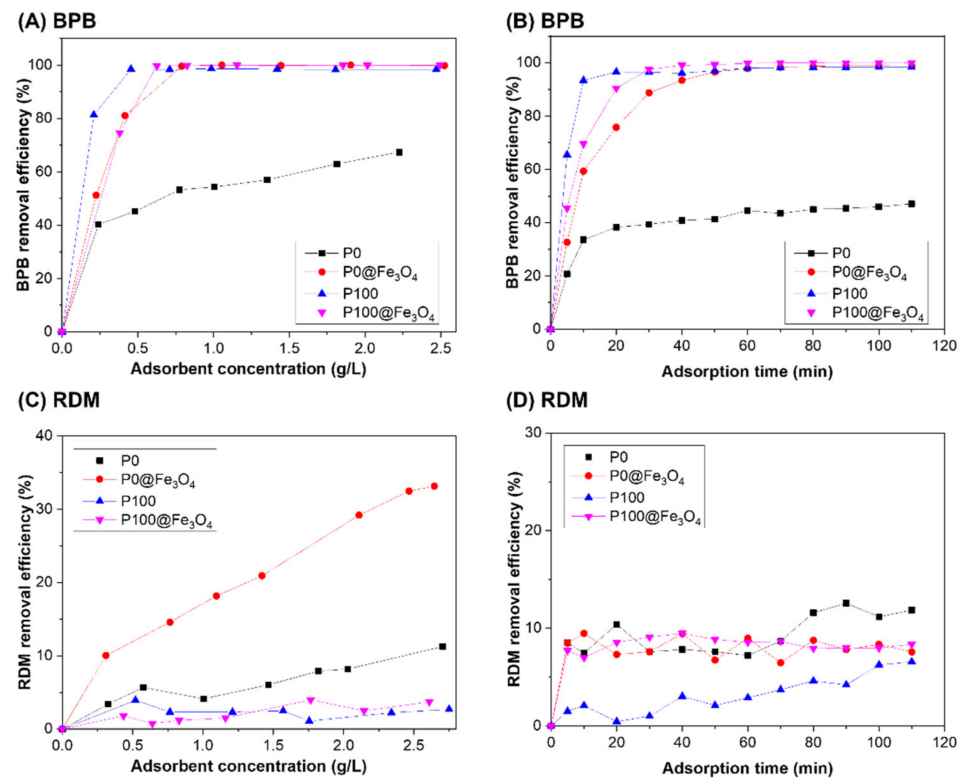


Figure 7. Graphs showing the removal efficiency of (A) BPB dye (0.5 mM, 350 mg/L) and (C) RDM dye (0.01 mM, 5 mg/L) as a function of adsorbent concentration for the hydrogels after 2 h of contact time. Graphs showing the removal efficiency of (B) BPB dye and (D) RDM dye as a function of adsorption time for the hydrogels. The adsorbent concentration was 0.42 g/L for the BPB solution (0.5 mM, 350 mg/L), and the adsorbent concentration was 0.62 g/L for the RDM solution (0.01 mM, 5 mg/L). All experimental data were measured at 25 °C.

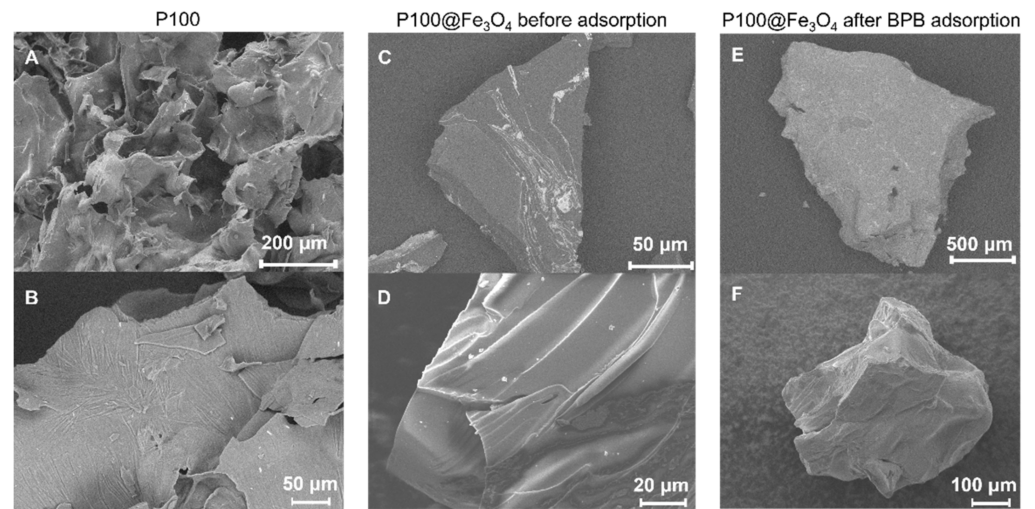


Figure 8. SEM images of (A,B) P100, (C,D) P100@Fe₃O₄ before adsorption, and (E,F) P100@Fe₃O₄ after BPB dye adsorption at different scales.

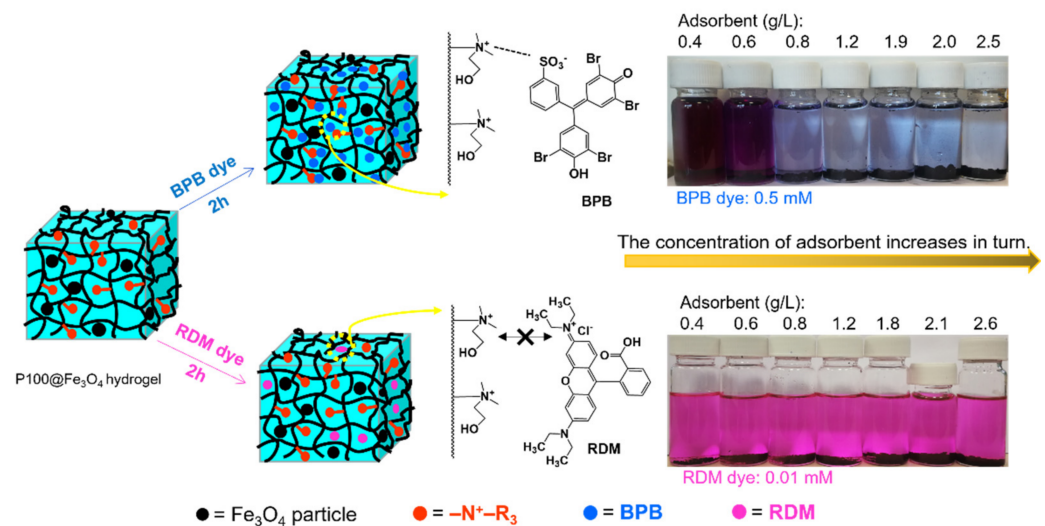


Figure 9. Schematic illustrations for BPB and RDM removal by P100@Fe₃O₄ hydrogel adsorbent.

The effect of chemical structures of the adsorbents on their dye removal efficiency and the BPB dye adsorption mechanism were also explored in the kinetics studies of BPB dye removal experiments (Figure 7B). The results showed that the removal efficiency of BPB dye increased with adsorption time, and the adsorption equilibrium was reached in approximately 30 min. The adsorption rate was very fast in the first 10 min, and the removal efficiency of BPB dye by P100 was over 90% in 20 min. The adsorption equilibrium was almost reached in 30 min, and the removal efficiency of BPB dye by P100 was 94%.

In contrast, the adsorption of RDM by these adsorbents was much less than BPB. At the maximum concentrations of P0, P0@Fe₃O₄, P100, and P100@Fe₃O₄ used in this experiment, the removal efficiency of RDM was only 11.3%, 33.2%, 2.7%, and 3.7%, respectively, as shown in Figure 7C. The removal efficiency of RDM by P0, P0@Fe₃O₄, P100, and P100@Fe₃O₄ with the adsorbent concentration of 0.62 g/L and RDM initial concentration of 5 mg/L was only 11.8%, 7.6%, 6.6%, and 8.4%, respectively (Figure 7D). The fundamental reason might be that RDM dye in aqueous solutions had positive charges and repelled each other with cationic hydrogel P100 and P100@Fe₃O₄, which was not conducive to dye adsorption. Moreover, the P0 hydrogel without cationic charge showed much better adsorption of RDM than P100, which further proved this hypothesis. The schematic illustration for RDM removal by magnetic hydrogel P100@Fe₃O₄ is shown in Figure 9.

The SEM image of the freeze-dried P100 particle in Figure 8A,B showed that the laminar structure was very obvious, and an irregular pore structure was present. This 3D porous structure could significantly increase the surface area of the hydrogel, which was conducive to accelerating dye adsorption. Figure 8C,D are the SEM images of the magnetic hydrogel P100@Fe₃O₄ particles before dye adsorption. The surface of the oven-dried P100@Fe₃O₄ particles was smooth and relatively nonporous without the 3D-layered structure of P100 hydrogel. The primary reason might be the formation of intermolecular hydrogen bonds among the –OH and CONH groups in hydrogel, inducing rapid shrinkage during in situ precipitation or the drying process. The SEM images of the oven-dried P100@Fe₃O₄ particles after BPB dye adsorption are shown in Figure 8E,F. Compared to P100@Fe₃O₄ before adsorption, its structure had no obvious change and it still had a smooth surface.

The kinetics data of the hydrogels were fitted into the pseudo-1st-order and pseudo-2nd-order models (Figure 10). The rate constants, k_1 and k_2 , and the q_e values are summarized in Table 2. The calculated results showed that the correlation coefficients (R^2) of the two models were quite different. The adsorption kinetics data of these adsorbents fitted better into the pseudo-2nd-order kinetic model ($R^2 > 0.99$), and the experimental q_e value and calculated q_e value from the pseudo-2nd-order kinetic model were also quite close. This indicates that BPB dye adsorption includes chemical adsorption and physical adsorption [21].

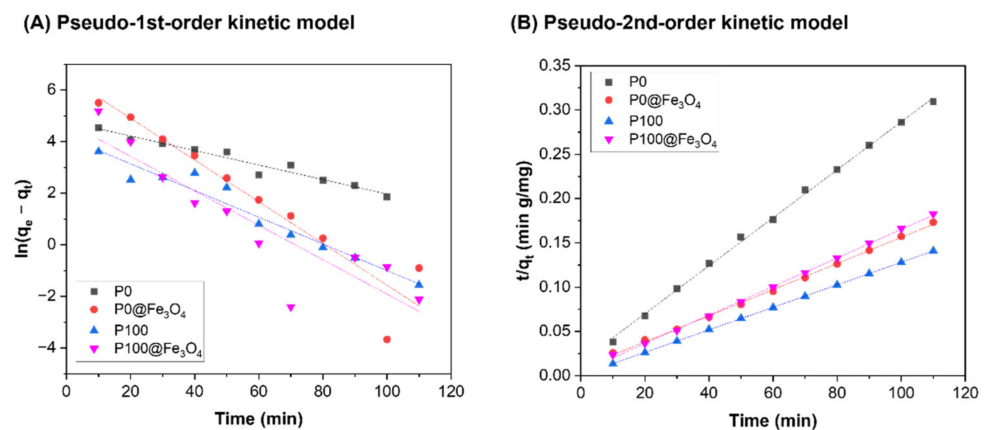


Figure 10. Linear fittings to the (A) pseudo-1st-order kinetic model and (B) pseudo-2nd-order kinetic model for adsorption of BPB by the hydrogels.

Table 2. Fitting parameters of adsorption kinetics of non-magnetic and magnetic hydrogels.

Adsorbents	Pseudo-1st-Order			Pseudo-2nd-Order			Experimental Values
	$q_{e,cal}$ (mg/g)	k_1 (L/mg)	R^2	$q_{e,cal}$ (mg/g)	k_2 (g/mg min)	R^2	$q_{e,exp}$ (mg/g)
P0	119.18	0.0281	0.9540	369.00	4.66×10^{-4}	0.9986	355.91
P100	65.04	0.0517	0.9475	787.40	1.85×10^{-3}	1.0000	781.33
P0@Fe ₃ O ₄	680.66	0.0809	0.9062	675.68	2.54×10^{-4}	0.9988	635.72
P100@Fe ₃ O ₄	117.06	0.0667	0.8197	621.12	6.43×10^{-4}	0.9993	602.75

3.4. Recycling Studies

The recycling studies of the hydrogels were conducted using 1 g/L of the adsorbents and 0.5 mM BPB solution at 25 °C. After adsorption of BPB, the desorption of BPB from the magnetic hydrogel P100@Fe₃O₄ and the non-magnetic hydrogel P100 was carried out in weakly acidic solutions (pH = 6) to regenerate the adsorbents before they were used again in the next cycles. The washing time needed to desorb BPB dye from the magnetic hydrogel P100@Fe₃O₄ and the non-magnetic hydrogel P100 was 2 and 5 min, respectively. The BPB

removal efficiency for five consecutive cycles of adsorption/desorption of the magnetic hydrogel P100@Fe₃O₄ and the non-magnetic hydrogel P100 are shown in Figure 11. These data show that these two adsorbents can be recycled and used for five times without a significant decrease in their BPB removal efficiency, which was 97.7% for P100 and 96.4% for P100@Fe₃O₄, respectively.

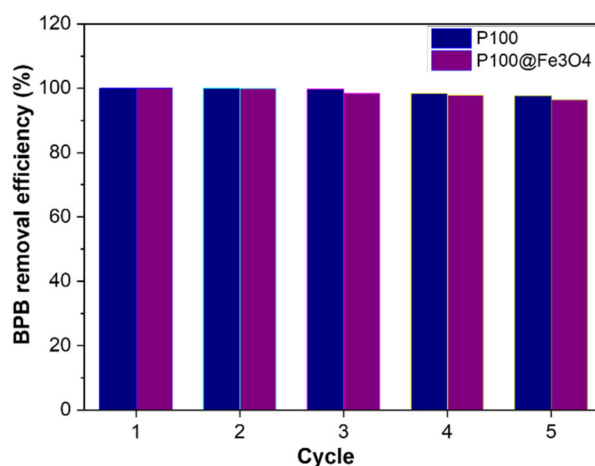


Figure 11. The BPB removal efficiency by P100 and P100@Fe₃O₄ hydrogels for five consecutive adsorption/desorption cycles at 25 °C.

4. Conclusions

In this study, the magnetic hydrogel, poly(DMAEAB-co-NIPAM)@Fe₃O₄, was successfully prepared and showed good selectivity for anionic dyes as an effective adsorbent for the removal of dye from aqueous solutions. The hydrogel poly(DMAEAB-co-NIPAM) was firstly synthesized, followed by incorporation of Fe₃O₄ into the hydrogel. The successful synthesized magnetic hydrogel was characterized by FTIR, XRD, TGA, and SEM. Subsequently, the adsorption behaviors of the non-magnetic and magnetic hydrogels were evaluated using BPB and RDM dyes. Various adsorption parameters, including adsorbent amount and adsorption time, were analyzed. The magnetic hydrogels showed an excellent BPB removal efficiency compared to the removal of RDM. The optimum adsorbent concentration for 0.5 mM BPB solution was approximately 0.5 g/L, and the removal efficiency was more than 99%. The kinetics data of BPB removal fitted well into the pseudo-2nd-order model, indicating that BPB dye adsorption involves chemical adsorption and physical adsorption. Furthermore, the reusability of the magnetic hydrogel for BPB removal was examined for up to five cycles and it could be reused without losing its high removal efficiency. The magnetic hydrogel, poly(DMAEAB-co-NIPAM)@Fe₃O₄, with high removal efficiency and good selectivity and reusability shows great potential for removal of anionic dyes in wastewater treatment.

Author Contributions: Conceptualization, Z.C., X.S. and J.L.; Methodology, Z.C., X.S. and J.L.; Investigation, Z.C., X.S., W.W.M.S., Y.W., J.Z. and M.Z.; Data curation, Z.C., X.S., W.W.M.S., Y.W., J.Z. and M.Z.; Writing—original draft preparation, Z.C. and X.S.; Writing—review and editing, Z.C., X.S. and J.L.; Supervision, J.L.; Funding acquisition, Z.C. and J.L. All authors have read and agreed to the published version of the manuscript.

Funding: The research was financially supported in part by Singapore’s Ministry of Education Academic Research Funds (grant Nos. R397000267114 and R397000296114), China’s Chongqing Municipal Science and Technology Commission (cstc2019jcyj-msxmX0232), and the Chongqing Municipal Education Commission (KJQN201801112).

Institutional Review Board Statement: Not applicable.

Informed Consent Statement: Not applicable.

Data Availability Statement: Data are available from the authors. Samples of the compounds are available from the authors.

Acknowledgments: Z.C. would like to acknowledge the financial support from the China Scholarship Council (No. 201708505114).

Conflicts of Interest: The authors declare no conflict of interest.

References

1. Tan, K.B.; Vakili, M.; Horri, B.A.; Poh, P.E.; Abdullah, A.Z.; Salamatinia, B. Adsorption of dyes by nanomaterials: Recent developments and adsorption mechanisms. *Sep. Purif. Technol.* **2015**, *150*, 229–242. [[CrossRef](#)]
2. Yagub, M.T.; Sen, T.K.; Afroze, S.; Ang, H. Dye and its removal from aqueous solution by adsorption: A review. *Adv. Colloid Interface Sci.* **2014**, *209*, 172–184. [[CrossRef](#)]
3. Ghaedi, M.; Ghaedi, A.M.; Khajehsharifi, H.; Yadkuri, A.H.; Roosta, M.; Asghari, A. Oxidized multiwalled carbon nanotubes as efficient adsorbent for bromothymol blue. *Toxicol. Environ. Chem.* **2012**, *94*, 873–883. [[CrossRef](#)]
4. Ghaedi, M.; Abdi, F.; Roosta, M.; Vafaei, A.; Asghari, A. Principal component analysis- adaptive neuro-fuzzy inference system modeling and genetic algorithm optimization of adsorption of methylene blue by activated carbon derived from Pistacia khinjuk. *Ecotoxicol. Environ. Saf.* **2013**, *96*, 110–117. [[CrossRef](#)]
5. Xu, Y.C.; Wang, Z.X.; Cheng, X.Q.; Xiao, Y.C.; Shao, L. Positively charged nanofiltration membranes via economically mussel-substance-simulated co-deposition for textile wastewater treatment. *Chem. Eng. J.* **2016**, *303*, 555–564. [[CrossRef](#)]
6. Khataee, A.R.; Vatanpour, V.; Ghadim, A.A. Decolorization of C.I. Acid Blue 9 solution by UV/Nano-TiO₂, Fenton, Fenton-like, electro-Fenton and electrocoagulation processes: A comparative study. *J. Hazard. Mater.* **2009**, *161*, 1225–1233. [[CrossRef](#)]
7. Basak, S.; Nandi, N.; Paul, S.; Hamley, I.W.; Banerjee, A. A tripeptide-based self-shrinking hydrogel for waste-water treatment: Removal of toxic organic dyes and lead (Pb²⁺) ions. *Chem. Commun.* **2017**, *53*, 5910–5913. [[CrossRef](#)]
8. Zhao, S.; Zhu, H.; Wang, Z.; Song, P.; Ban, M.; Song, X. A loose hybrid nanofiltration membrane fabricated via chelating-assisted in-situ growth of Co/Ni LDHs for dye wastewater treatment. *Chem. Eng. J.* **2018**, *353*, 460–471. [[CrossRef](#)]
9. Aleboye, A.; Kasiri, M.; Olya, M. Prediction of azo dye decolorization by UV/H₂O₂ using artificial neural networks. *Dye. Pigment.* **2008**, *77*, 288–294. [[CrossRef](#)]
10. Tomé, L.C.; Gouveia, A.S.; Freire, C.; Mecerreyes, D.; Marrucho, I. Polymeric ionic liquid-based membranes: Influence of polycation variation on gas transport and CO₂ selectivity properties. *J. Membr. Sci.* **2015**, *486*, 40–48. [[CrossRef](#)]
11. Esmaeli, A.; Jokar, M.; Kousha, M.; Daneshvar, E.; Zilouei, H.; Karimi, K. Acidic dye wastewater treatment onto a marine macroalga, Nizamuddina zanardini (Phylum: Ochrophyta). *Chem. Eng. J.* **2013**, *217*, 329–336. [[CrossRef](#)]
12. Shen, C.; Shen, Y.; Wen, Y.; Wang, H.; Liu, W. Fast and highly efficient removal of dyes under alkaline conditions using magnetic chitosan-Fe(III) hydrogel. *Water Res.* **2011**, *45*, 5200–5210. [[CrossRef](#)]
13. Yao, W.; Rao, P.; Zhang, W.; Li, L.; Li, Y. Preparation of Thermo-Sensitive Magnetic Cationic Hydrogel for the Adsorption of Reactive Red Dye. *J. Dispers. Sci. Technol.* **2015**, *36*, 714–722. [[CrossRef](#)]
14. Kuroiwa, T.; Takada, H.; Shogen, A.; Saito, K.; Kobayashi, I.; Uemura, K.; Kanazawa, A. Cross-linkable chitosan-based hydrogel microbeads with pH-responsive adsorption properties for organic dyes prepared using size-tunable microchannel emulsification technique. *Colloids Surf. A Physicochem. Eng. Asp.* **2017**, *514*, 69–78.
15. Stanciu, M.C.; Nichifor, M. Adsorption of anionic dyes on a cationic amphiphilic dextran hydrogel: Equilibrium, kinetic, and thermodynamic studies. *Colloid Polym. Sci.* **2018**, *297*, 45–57. [[CrossRef](#)]
16. Stanciu, M.C.; Nichifor, M. Influence of dextran hydrogel characteristics on adsorption capacity for anionic dyes. *Carbohydr. Polym.* **2018**, *199*, 75–83. [[CrossRef](#)]
17. Song, X.; Mensah, N.N.; Wen, Y.; Zhu, J.; Zhang, Z.; Tan, W.S.; Chen, X.; Li, J. β -Cyclodextrin-Polyacrylamide Hydrogel for Removal of Organic Micropollutants from Water. *Molecules* **2021**, *26*, 5031. [[CrossRef](#)]
18. Liu, M.; Wen, Y.; Song, X.; Zhu, J.-L.; Li, J. A smart thermoresponsive adsorption system for efficient copper ion removal based on alginate-g-poly(N-isopropylacrylamide) graft copolymer. *Carbohydr. Polym.* **2019**, *219*, 280–289. [[CrossRef](#)]
19. Zhu, H.-Y.; Fu, Y.-Q.; Jiang, R.; Yao, J.; Xiao, L.; Zeng, G.-M. Novel magnetic chitosan/poly(vinyl alcohol) hydrogel beads: Preparation, characterization and application for adsorption of dye from aqueous solution. *Bioresour. Technol.* **2012**, *105*, 24–30. [[CrossRef](#)] [[PubMed](#)]
20. Eftekhari-Sis, B.; Rahimkhoei, V.; Akbari, A.; Araghi, H.Y. Cubic polyhedral oligomeric silsesquioxane nano-cross-linked hybrid hydrogels: Synthesis, characterization, swelling and dye adsorption properties. *React. Funct. Polym.* **2018**, *128*, 47–57. [[CrossRef](#)]
21. Huang, H.; Hou, L.; Zhu, F.; Li, J.; Xu, M. Controllable thermal and pH responsive behavior of PEG based hydrogels and applications for dye adsorption and release. *RSC Adv.* **2018**, *8*, 9334–9343. [[CrossRef](#)]
22. Kumar, N.; Mittal, H.; Alhassan, S.; Ray, S.S. Bionanocomposite Hydrogel for the Adsorption of Dye and Reusability of Generated Waste for the Photodegradation of Ciprofloxacin: A Demonstration of the Circularity Concept for Water Purification. *ACS Sustain. Chem. Eng.* **2018**, *6*, 17011–17025. [[CrossRef](#)]
23. Li, D.; Li, Q.; Bai, N.; Dong, H.; Mao, D. One-Step Synthesis of Cationic Hydrogel for Efficient Dye Adsorption and Its Second Use for Emulsified Oil Separation. *ACS Sustain. Chem. Eng.* **2017**, *5*, 5598–5607. [[CrossRef](#)]

24. AlOkour, M.; Yilmaz, E. Photoinitiated synthesis of poly(poly(ethylene glycol) methacrylate- co -diethyl amino ethyl methacrylate) superabsorbent hydrogels for dye adsorption. *J. Appl. Polym. Sci.* **2019**, *136*, 47707. [[CrossRef](#)]
25. Qi, X.; Wu, L.; Su, T.; Zhang, J.; Dong, W. Polysaccharide-based cationic hydrogels for dye adsorption. *Colloids Surf. B Biointerfaces* **2018**, *170*, 364–372. [[CrossRef](#)] [[PubMed](#)]
26. Kwon, I.C.; Bae, Y.H.; Kim, S.W. Electrically erodible polymer gel for controlled release of drugs. *Nat. Cell Biol.* **1991**, *354*, 291–293. [[CrossRef](#)]
27. Yang, C.; Wang, W.; Yao, C.; Xie, R.; Ju, X.-J.; Liu, Z.; Chu, L.-Y. Hydrogel Walkers with Electro-Driven Motility for Cargo Transport. *Sci. Rep.* **2015**, *5*, 13622. [[CrossRef](#)] [[PubMed](#)]
28. Song, X.; Zhang, Z.; Zhu, J.; Wen, Y.; Zhao, F.; Lei, L.; Phan-Thien, N.; Khoo, B.C.; Li, J. Thermoresponsive Hydrogel Induced by Dual Supramolecular Assemblies and Its Controlled Release Property for Enhanced Anticancer Drug Delivery. *Biomacromolecules* **2020**, *21*, 1516–1527. [[CrossRef](#)]
29. Liu, M.; Song, X.; Wen, Y.; Zhu, J.-L.; Li, J. Injectable Thermoresponsive Hydrogel Formed by Alginate-g-Poly(N-isopropylacrylamide) That Releases Doxorubicin-Encapsulated Micelles as a Smart Drug Delivery System. *ACS Appl. Mater. Interfaces* **2017**, *9*, 35673–35682. [[CrossRef](#)]
30. Zhou, A.; Chen, W.; Liao, L.; Xie, P.; Zhang, T.C.; Wu, X.; Feng, X. Comparative adsorption of emerging contaminants in water by functional designed magnetic poly(N-isopropylacrylamide)/chitosan hydrogels. *Sci. Total Environ.* **2019**, *671*, 377–387. [[CrossRef](#)]
31. Parasuraman, D.; Serpe, M.J. Poly (N-Isopropylacrylamide) Microgels for Organic Dye Removal from Water. *ACS Appl. Mater. Interfaces* **2011**, *3*, 2732–2737. [[CrossRef](#)]
32. Song, X.; Zhu, J.-L.; Wen, Y.; Zhao, F.; Zhang, Z.-X.; Li, J. Thermoresponsive supramolecular micellar drug delivery system based on star-linear pseudo-block polymer consisting of β -cyclodextrin-poly(N-isopropylacrylamide) and adamantyl-poly(ethylene glycol). *J. Colloid Interface Sci.* **2017**, *490*, 372–379. [[CrossRef](#)]
33. Song, X.; Wen, Y.; Zhu, J.-L.; Zhao, F.; Zhang, Z.-X.; Li, J. Thermoresponsive Delivery of Paclitaxel by β -Cyclodextrin-Based Poly(N-isopropylacrylamide) Star Polymer via Inclusion Complexation. *Biomacromolecules* **2016**, *17*, 3957–3963. [[CrossRef](#)]
34. Diao, B.; Zhang, Z.; Zhu, J.; Li, J. Biomass-based thermogelling copolymers consisting of lignin and grafted poly(N-isopropylacrylamide), poly(ethylene glycol), and poly(propylene glycol). *RSC Adv.* **2014**, *4*, 42996–43003. [[CrossRef](#)]
35. Zhang, Z.-X.; Liu, K.L.; Li, J.A. Thermoresponsive Hydrogel Formed from a Star-Star Supramolecular Architecture. *Angew. Chem. Int. Ed.* **2013**, *52*, 6180–6184. [[CrossRef](#)]
36. Atta, A.M.; Al-Hussain, S.A.; Al-Lohedan, H.A.; Ezzat, A.O.; Tawfeek, A.M.; Al-Otobi, T. In situ preparation of magnetite/cuprous oxide/poly(AMPS/NIPAm) for removal of methylene blue from waste water. *Polym. Int.* **2018**, *67*, 471–480. [[CrossRef](#)]
37. Atta, A.M.; Hameed, R.S.A.; Al-Lohedan, H.A.; Ezzat, A.O.; Hashem, A.I. Magnetite doped cuprous oxide nanoparticles as modifier for epoxy organic coating. *Prog. Org. Coat.* **2017**, *112*, 295–303. [[CrossRef](#)]
38. Karthika, J.; Vishalakshi, B. Novel stimuli responsive gellan gum-graft-poly(DMAEMA) hydrogel as adsorbent for anionic dye. *Int. J. Biol. Macromol.* **2015**, *81*, 648–655. [[CrossRef](#)] [[PubMed](#)]
39. Alorabi, A.Q.; Shamshi Hassan, M.; Azizi, M. Fe₃O₄-CuO-activated carbon composite as an efficient adsorbent for bromophenol blue dye removal from aqueous solutions. *Arab. J. Chem.* **2020**, *13*, 8080–8091. [[CrossRef](#)]